CHAPTER

14

Integration of Experimental and Computational Microfluidics in 3D Tissue Engineering

Manuela T. Raimondi,[1,2] Devin T. Bridgen,[3] Matteo Laganà,[1,2] Beatrice Tonnarelli,[3] Margherita Cioffi,[1,2] Federica Boschetti,[1,2] and David Wendt[3]

[1]LaBS, Department of Structural Engineering, Politecnico di Milano, Milano, Italy, [2]IRCCS Galeazzi Orthopaedic Institute, Milano, Italy, [3]Departments of Surgery and of Biomedicine, University Hospital Basel, Basel, Switzerland, corresponding author: Manuela Teresa Raimondi, address: Laboratory of Biological Structure Mechanics (LaBS), Department of Structural Engineering, Politecnico di Milano, 32, piazza Leonardo da Vinci, 30133 Milano, Italy, phone: +39.02.2399.4306, e-mail: manuela.raimondi@polimi.it

Abstract

We present an integrated system, combining computational flow analysis with a microbioreactor designed for three-dimensional (3D) scaffolds to study the effects of hydrodynamic conditions on cell behavior over time. Using appropriate staining and imaging protocols, thin cell-seeded 3D scaffolds with a controlled architecture are monitored nondestructively in time and space. Computational fluid dynamic (CFD) simulation quantifies the fluidic environment within the scaffold pores. The model geometry and boundary conditions directly correspond to the environment given by the flow channel and specific scaffold architecture. Integrating the computational and experimental data, local fluid conditions are correlated one-to-one with local cell behavior throughout the course of culture. This concept is illustrated using the microfluidic system to investigate the effect of shear stress on cell proliferation in 3D. We explore design considerations and potential applications in tissue engineering for studying the cell response in a perfused 3D environment.

Key terms: bioreactor, cell proliferation, computational model, imaging, interstitial perfusion, microfluidics, shear stress, tissue engineering

14.1 Introduction

In the design of 3D porous biomaterials to serve as implants in tissue engineering, a central concern is the control of mass transport. While scaffold material properties, surface chemistry, and degradation behavior are important, the transport of gases and nutrients to cells and of catabolites away from cells is now established as the crucial factor affecting cell survival [1]. Tissue engineering may use fluid flow to respond to mass transport limitations; the cell-seeded scaffold is immersed in a culture medium, which is induced to flow through the scaffold structure in interstitial perfusion bioreactors.

In scaffold-based cartilage regeneration, the interstitial fluid flow of culture medium is believed to be particularly effective in up-regulating the biosynthesis of matrix proteins, as it results in cell membrane stretching, due to fluid-induced shear, and in the convection-enhanced transport of solutes [2]. Under interstitial perfusion, a simple means of increasing mass transport to cells would be to increase the medium flow rate. High flow rates induce high shear stresses on cells, which may be harmful instead of beneficial at all stages of tissue growth. We address the issue by establishing quantitative relationships between the field variables of the fluid dynamic field imposed to cells, and the cell response within the 3D tissue.

Flow around constructs in a bioreactor may be computed in terms of flow fields, shear stresses, and oxygen profiles, through the use of a computational fluid dynamic (CFD) model [3]. Incorporating flow through the scaffold in an interstitial-perfusion configuration complicates the situation by establishing a velocity scale that is related to the actual fluid velocities in the scaffold, which are not experimentally accessible and are thus impossible to measure. This complex problem is investigated by the use of detailed pore-scale CFD simulations of fluid and the solute transport in tissue engineering scaffolds [4–8]. CFD numerical techniques are able to capture flow, pressure, and concentration fields resolved at the scaffold's pore level. Calculations indicate that inappropriately designed dynamic culture environments lead to regions of harmful shear stresses or nutrient concentrations insufficient to maintain cell viability [9].

So far, attempts to calculate and control the balance of mass transport/shear stress by proper selection of medium flow rate and scaffold microgeometry have proven useful in capturing a rough understanding of the conditions favoring the initial development of engineered tissues such as bone [10] and cartilage [11–14]. These efforts have been directed towards the establishment of a quantitative correlation between levels of shear stress, obtained by averaging out the wide range of imposed shears into a single shear level value, and construct parameters such as cellularity or the change in matrix protein expression. However, the local shear stresses are widely heterogeneous [6], making correlations between shear level and effects on matrix composition very difficult to assess. A step forward in this regard would be the establishment of variable correlation as a function of spatial location. More specifically, a point-by-point correlation is generated between the local field variables calculated for the fluid dynamic field within the construct, and the biosynthetic response measured at the celularl level within the 3D construct.

The complexity of the 3D system and the associated limitations of the destructive and off-line analyses on the cellular constructs are overcome through the use of an advanced microfluidic model. This model allows nondestructive online monitoring of local parameters of the construct during perfusion culture. Microfluidic systems have rapidly gained popularity for use in cell culture, as shown by several recent examples of

studying angiogenesis [15], axonal guidance [16], liver tissue engineering [17, 18], bone differentiation [19], and stem cell differentiation [20]. Microfluidic systems provide the capability to control many of the critical biochemical and biophysical factors, allow for the culture of a wide range of cell types, and can be imaged in real time at high resolution. For example, one can seed a cell type in a microchamber and examine the local response to time-dependent flows and the delivery of mechanical stimuli and growth factors. These capabilities have opened new perspectives to tissue engineering studies that were not previously possible with a conventional bioreactor system.

We have developed an integrated experimental/computational microfluidic model of in vitro–engineered cartilaginous tissue. The tissue model consists of a construct made of chondrocytes seeded on a porous 3D scaffold. The CFD simulations quantify the local shear stress distribution within the perfused scaffold microarchitecture. By using a 3D scaffold with a simple and well-defined architecture, the CFD model is dramatically simplified and more readily compared to the experimental data.CFD is used initially to help define an appropriate 3D scaffold structure, which will generate significant local variations of fluid-induced shear stress within the porous architecture when perfused. A microfluidic bioreactor is developed, allowing the online monitoring of the construct during perfusion culture. A quantitative correlation is established by the CFD simulationbetween the experimental data from cell cultures and the geometric configuration of the microbioreactor.

14.2 Experimental Design

The integration of computational and experimental data elucidates the effect of local shear stresses, induced by specific perfusion conditions and scaffold architecture, on local cell behavior over time under an interstitial perfusion. Specifically, we aim to quantify the proliferation of cells within defined regions of the scaffold microarchitecture. Different perfusion velocities are used to induce varying magnitudes of shear, with the local shear stress quantified by a pore-scale CFD simulation. The microfluidic model consists of a microbioreactor in which a thin 3D cellular construct, 500 μm in thickness, is cultured under an interstitial perfusion. The bioreactor allows nondestructive online monitoring of cells cultured under perfusion, drastically reducing the sample size needed to acquire statistically significant data when taking destructive time points. Confocal and fluorescent time lapse microscopy (nondestructive) is used to monitor local cell distribution within specific locations of the scaffold over the time course of the culture.

14.3 Materials

14.3.1 Solutions

- Complete medium (CM): Dulbecco's modified Eagle's medium (DMEM) (Gibco-BRL), 10% fetal bovine serum (FBS) (Gibco-BRL), 1-mM Sodium Pyruvate (Gibco-BRL), 10-mM HEPES buffer (Gibco-BRL), 1% penicillin/streptomycin/glutamine (PSG)(Gibco-BRL). Store at 4°C.

- Growth medium (GM): Complete medium with 1 ng/ml TGFβ-1 (R&D Systems) and 5 ng/ml FGF2 (R&D Systems). Store at 4°C.
- 1× phosphate-buffered saline (PBS) (Gibco-BRL). Store at 4°C.
- DAPI (Sigma)
- SYTO 13 (Sigma)
- Ethedium Homodimer 1, from LIVE/DEAD viability kit (Juro)

14.3.2 Disposables

- Glass microscope slides, 40 mm × 26 mm × 0.2 mm (Assistent)
- Platinum cured silicone tubing, 0.8 mm ID (Fisher Scientific)
- Uncoated 8-well microscopy micro slides (Ibidi)
- Coverwell microperfusion chambers (Grace Bio Labs, PC3L-0.5)
- Silicone rubber gaskets (Maagtechnic)

14.3.3 Equipment

- Roller pump (Ismatec)
- Syringe pump (Harvard Apparatus)
- Incubators set at 37°C, 5% CO_2
- Confocal microscope (LSM 710, Carl Zeiss)

14.3.4 Custom equipment

- Perfusion cell seeding system
- Microbioreactor
- 8 × 3 × 0.5 mm polystyrene scaffolds (3D Biotek)

14.3.5 Software

- Gambit (Ansys), ACIS-based solid modeler
- FLUENT (Ansys), CFD code
- SolidWorks (Dassault Systèmes SolidWorks Corp), 3D CAD design software
- Zen (Carl Zeiss), 3D reconstruction software

14.4 Methods

In this section the methods used to build an integrated experimental/computational microfluidic model to monitor local cell proliferation in relation to local shear stress are detailed. While these methods are quite specific, the general concept can be used for many different applications. Therefore, general design considerations are given in Section 14.6.

14.4.1 Microfluidic chamber design

1. The microfluidic bioreactor is designed in coordination with the specific geometry of the 3D scaffold. To ensure a strong correlation with the computational model, it is critical that the scaffold has a well-defined architecture. Rapid prototype polystyrene scaffolds with a plasma surface treatment, custom-made by 3D Biotek, are used in the proliferation experiments (Figure 14.1). The fibers are 100 μm in diameter with a pore size of 300 μm and stacked in an offset cross-hatch geometry. The overall geometry is 8 mm $\times$ 3 mm $\times$ 0.5 mm.
2. The bioreactor must be sterile while allowing easy insertion of the scaffold. It is for this reason that a sandwich design is used (Figure 14.2).
3. Once the individual bioreactor is assembled, the inlet and outlet ports are connected to the media reservoir with silicone tubing. To ensure accurate flow rates, each channel is perfused individually. The growth media can be perfused with a peristaltic pump circulating the media in a loop, or with a syringe pump for lower flow rates (Figure 14.3).

14.4.2 Computational model

1. Set up the model geometry and mesh. The ACIS-based, solid modeler Gambit is used here. Reconstruct the scaffold geometry and dimensions (Figure 14.1). Determine the existing symmetries and study only a fraction of the model to limit the computational cost (e.g., one-fourth of the model is studied here). Use a 4-node-tetrahedral mesh. Provide a number of elements and element spacing that will enable a resolution at the scaffold walls of areas smaller than a cell (<20–25 μm). Use a sufficiently fine mesh to resolve the boundary layer and the corresponding

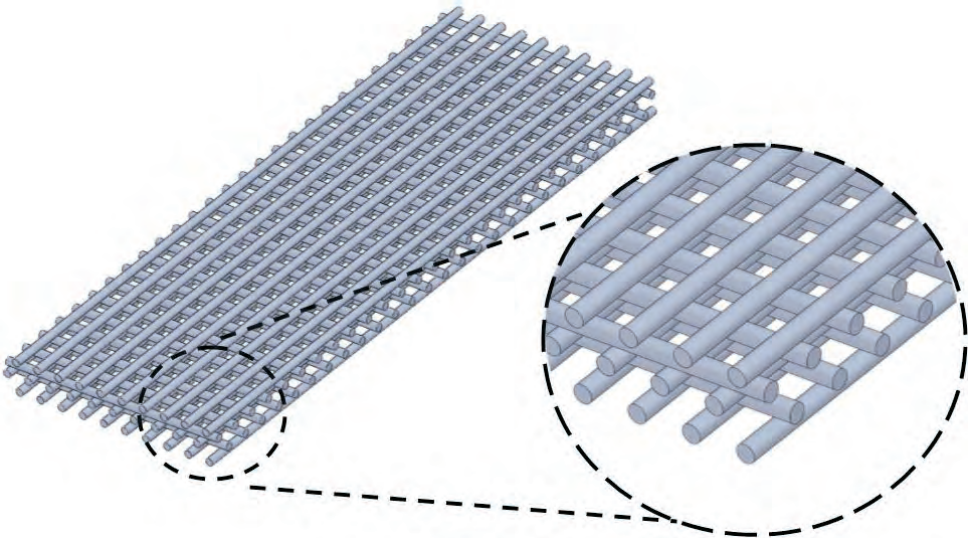

Figure 14.1 Scaffold geometry used for proliferation data. The fiber diameter is 100 μm and the pore size is 300 μm. The overall dimension of the scaffold is 3 mm $\times$ 8 mm $\times$ 0.5 mm.

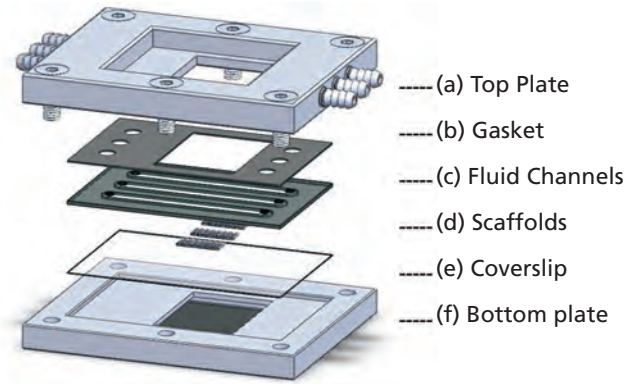

Figure 14.2 Expanded view of the microfluidic chamber. The (a) top and (f) bottom plates provide structural support and provide the pressure, using screws, to compress the assembly enough that there are no fluid leaks and sterility is maintained. It is important that they maintain a low profile so that they fit comfortably under a microscope and the objective can reach the cover slip. Our plates were custom machined out of stainless steel. The top plate contains small channels moving fluid from the threaded luer locks to the corresponding holes in the gasket below. (b) The gasket is used to ensure a tight seal between the top plate and the polycarbonate top of the flow channels. Holes on each end of the gasket allow fluid to flow from channels in the top plate, through the holes in the polycarbonate plate, and into the perfusion chamber. (c) The fluid channels are made from medical grade silicone bonded to clear, UV-transparent polycarbonate plastic. Channels in the silicone define the flow channel architecture, with fluid constrained by the cover slip and polycarbonate on the top and bottom and by the silicone on the sides. (d) The scaffolds are inserted between the cover slip and the perfusion chamber. When the top and bottom plates are screwed together, the pressure slightly compresses the silicone in the perfusion chamber, ensuring a tight fit for the scaffolds. (e) The cover slip thickness balances the structural strength with an optical efficiency when imaging, and we have found that a 0.2-mm thickness works well. This is a fragile portion of the bioreactor, and care must be taken when moving the objective of a microscope so that you do not break the cover slip. The chamber adheres to the cover slip below, providing a water-tight channel. Our design uses three 0.5-mm-thick channels per bioreactor (cat no. PC3L-0.5).

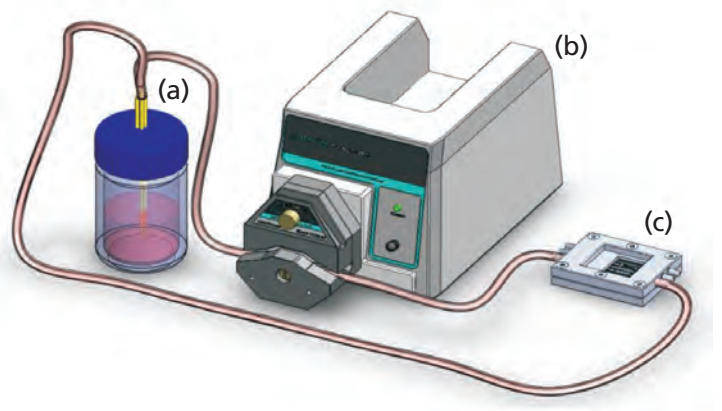

Figure 14.3 Diagram showing the full setup of the microbioreactor. (a) Culture medium reservoir. (b) Peristaltic pump. (c) Microfluidic chamber. Only one set of tubing is shown for simplicity, when in reality there are three sets per bioreactor. A filter and septum are attached to the media reservoir for, respectively, gas and media exchange.

shear stress distribution at the scaffold wall surfaces. It is also possible to discretize the fluid field with a mesh progressively refined near the scaffold walls. Here the mesh consists of 246,600 elements.

2. Set up and solve the fluid dynamic problem. The commercial finite-volume code FLUENT is used here.
   a. Set the boundary conditions. Apply no-slip boundary conditions to the solid surfaces representing the scaffold fibers under the hypothesis of rigid, impermeable walls. Impose a flat velocity profile at the inlet. The applied velocity (in the described example, 100 μm/s) will correspond to the flow rate experimentally applied through the scaffold. Apply null total stress at the outlet. Use symmetry boundary conditions for the lateral sides of the fluid domain and no-slip boundary conditions for the upper and lower surfaces of the domain.
   b. Model the fluid. Model the culture medium at 37°C as an incompressible, homogeneous, Newtonian fluid with a density equal to 1,000 kg m^{-3}. The viscosity, measured for Dulbecco's Modified Eagle Medium at 37°C, is 8.2×10^{-4} kg $m^{-1}s^{-1}$ [11].
   c. Run the simulations. The equations solved by FLUENT are the steady-state Navier-Stokes equations. Choose a segregated solver for the solution method and a conjugate gradient-based iterative solver to solve the symmetric and nonsymmetric linear systems. Here, computations are carried out on a Windows NT PC with 2-Gb RAM.
3. Analyze the results. Determine the fluid velocity magnitudes and the distribution of wall shear stress at the scaffold walls. Process wall shear stress data at the pore level to obtain the maximum, minimum, and average values, which are an estimate of the shear stress range induced at the scaffold walls.
4. Calculate the Reynolds number. Use the equation $\mathrm{Re} = d\rho v/\mu$, where d is the hydraulic diameter, equal to 4 × fluid volume/surface area, ρ is the fluid density, v is the average inlet velocity, and μ is the fluid viscosity. Reynolds numbers are typically very low in interstitial perfusion bioreactors (e.g., here $\mathrm{Re} = 10^{-3}$); thus, the convective terms of the fluid dynamic equations are negligible and the shear stress is linearly related to the imposed inlet flow rate. Use the calculated shear stresses to extrapolate shear stress levels for different inlet velocities.

14.4.3 Dynamic scaffold seeding

1. If not presterilized by the manufacturer, submerse the scaffolds in isopropyanol for 10 minutes, followed by three 10-minute washes and an overnight soak in DMEM at 37°C.
2. To obtain a uniform distribution of cells throughout the scaffold, cells may be seeded under perfusion in a bioreactor, as previously described [1]. It is necessary to use a low cell number, since a higher cell density could alter the scaffold pore architecture and compromise correlations to the computational model.
3. To determine the appropriate number of cells to seed, perform preliminary seeding experiments. For the 3D Biotek scaffold, having a seeding efficiency of about 10%, inject 100,000 cells per scaffold.
4. Perfuse the cell suspension through the scaffold overnight. If the fluid velocity is too high, cells may not attach to the scaffold. However, if the fluid velocity is too slow, a majority of the cells will adhere elsewhere in the bioreactor, significantly decreasing seeding efficiency. A fluid velocity of ~1,000 μm/s was used for the seeding.

14.4.4 Microbioreactor setup

1. The bioreactor is designed so that each component, aside from the scaffold, can be autoclaved.
2. While under sterile conditions, carefully take the scaffolds out of the perfusion seeding system. It is important to be gentle with the scaffolds to prevent cell detachment. Place each scaffold in CM.
3. Perform cell nuclear staining with DAPI at a concentration of 10 μg/ml. The staining protocol is as follows:
   a. Dissolve DAPI in deionized water to make a stock concentration of 5 mg/ml. Since DAPI is not very soluble, try sonicating the solution in addition to 5 minutes of vortexing.
   b. Combine 1× PBS with stock DAPI to form a 10 μg/ml solution.
   c. Incubate the constructs in the solution for 90 minutes at 37°C.
   d. Wash the constructs twice with 1× PBS before resubmerging in CM.
4. Attach silicone tubing to each inlet/outlet on the bioreactor and to the media reservoir, which has already been filled with GM. If using a syringe pump, prefill the syringe and tubing with media before attaching to the bioreactor.
5. Place the glass cover slip on the top of the bottom plate of the bioreactor.
6. Place the scaffolds with stained cells into the perfusion chambers. Work quickly so that the scaffolds do not dry out.
7. Place the flow channels onto the cover slip.
8. Place the gasket onto the flow channels, taking care to align the holes for fluid flow.
9. Place the top plate on top of the gasket, insert the screws, and tighten the top plate against the bottom plate.
10. Briefly start the pump to fill the fluid channels with media, preventing the scaffolds from becoming dry.
11. Select the desired flow rate (e.g., 100 μm/s and 1 μm/s) and start the pump, creating a fluid flow through the bioreactor which perfuses the scaffold (Figure 14.4). A static control is kept in a 6-well plate with a comparable volume of media so that the nutrient supply is not the limiting factor. The final setup should look similar to that shown in Figure 14.3.

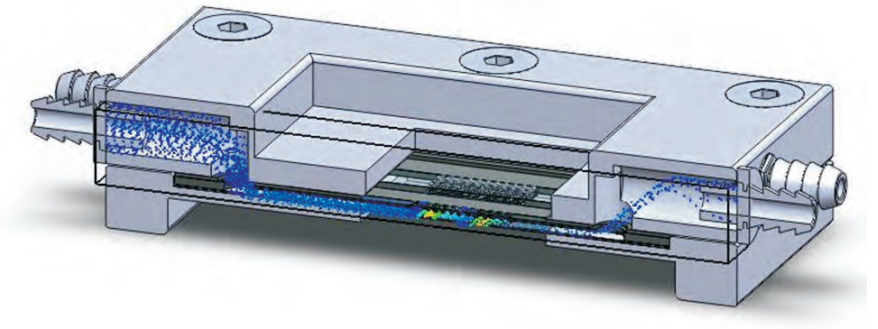

Figure 14.4 Cutaway of the microfluidic chamber. It shows the flow path of the growth media while being perfused at an average velocity of 100 μm/sec.

14.4.5 Imaging and data acquisition

1. For each desired time point, move the bioreactors to the confocal microscope. For long durations, it is advisable to use a heated environmental chamber to hold the bioreactor while taking images. A confocal microscope allows you to obtain the 3D information needed to take full advantage of the proposed design. A 10× objective with the aperture set at 1 airy unit, corresponding to an image depth of about 10 μm, is used for imaging. Using the features "tile scan" and "auto z," z-stacks in adjacent blocks are stitched together forming one large image.
2. At the final time point, an additional destructive analysis can supplement the previous data. Specifically, to look at local cell viability, the following live/dead assay protocol can be used:
   a. Stain the cell nuclei by submersing the scaffolds in 5-μM SYTO-13 Dye diluted in CM. Incubate the scaffolds for 90 minutes at 37°C, and then rinse once with 1× PBS.
   b. Stain the nuclei of the dead cells with 5-μM ethidium homodimer-1 (EthD-1), diluted in 1× PBS. Incubate for 30 minutes at 37°C, and then rinse with 1× PBS.
   c. Place the scaffolds in the 8-well microslides and submerse in 1× PBS. Image the cells.
3. Using Zen software, cells can be counted in both the high shear and low shear zones on the scaffold. It is important to have well-defined regions to compare. For the fiber-based scaffold from 3D Biotek, count the cells along a horizontal cross section of a fiber and compare it to a vertical cross section. This is described in more detail in Section 14.5.
4. To assess the total number of cells within the scaffold, detach the cells with collagenase and trypsin and manually count.

14.5 Anticipated Results and Interpretation

The results of the computational simulations allow quantification of the local flow field inside the scaffold (Figure 14.5) and the distribution of the wall shear stresses on the scaffold fibers (Figure 14.6). The local heterogeneity in the velocity and shear stress results is induced by the scaffold microstructure and the geometry of the microbioreactor channels. Therefore, with a different combination of channel and scaffold geometries, different results may be obtained. For the scaffold-microbioreactor system described here, at an applied inlet velocity of 100 μm/s, velocity magnitudes range from 0 to 370 μm/s and shear stress magnitudes range from 0 to 21 mPa.

The heterogeneous local fluid flow induces inhomogeneity in wall shear stresses, which are proportional to the velocity gradients. The lowest wall shear stresses are found at the fiber intersections, where the flow penetration is poor: the average shear stress in these areas is about 2 mPa (Figure 14.6). Conversely, the highest shear stresses are computed on the fibers oriented perpendicularly to flow, with peak values at the surfaces oriented parallel to to the top and bottom planes of the microbioreactor channels. In general, for a given scaffold, the thinner the microbioreactor channel, the bigger the difference between minimum and maximum shear stresses. Similarly, for a given

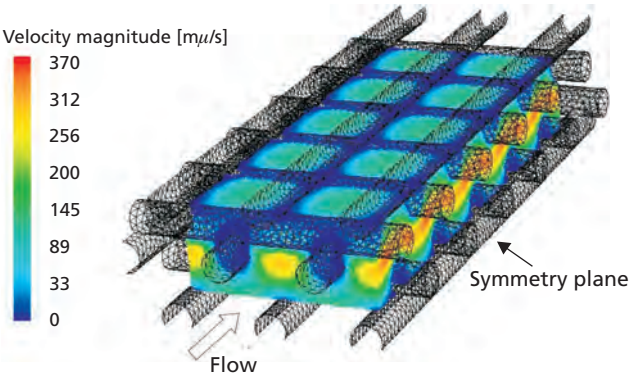

Figure 14.5 Results of CFD modeling. Calculated fluid velocity field mapped in the 3D scaffold perfused at an inlet velocity of 100 μm/s.

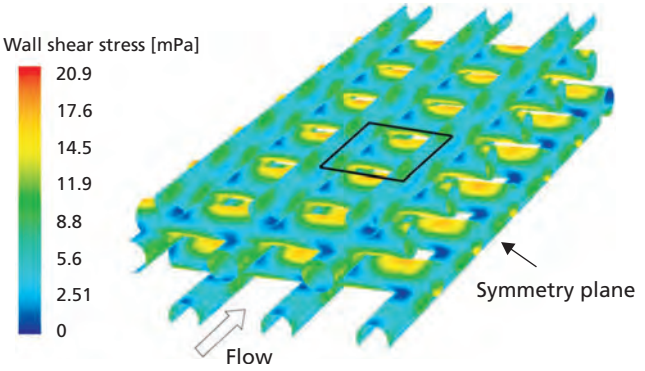

Figure 14.6 Results of CFD modeling. Calculated wall shear stress field mapped on the surfaces of the 3D scaffold perfused at an inlet velocity of 100 μm/s. The black square indicates the detail shown in the top view in Figure 14.8(b).

bioreactor chamber, the smaller the scaffold pores, the higher the expected maximum wall shear stress.

Using the given experimental protocol, a 3D reconstruction of your entire scaffold, as shown in Figure 14.7, can be obtained. Focusing on individual pores, a representative output of our method is shown in Figure 14.8. Overlapping the confocal image [Figure 14.8(a)] to the computed shear stress map [Figure 14.8(b)] gives the correlation between the computational and experimental outputs [Figure 14.8(c)]. Using this information, it is possible to clarify which specific regions would be most appropriate to compare. While a 3D reconstruction of the z stacks provides excellent qualitative data, it must be further modified for accurate quantitative analysis. It is critical that you select precisely defined voxels to compare in order to prevent bias. Each confocal image, while literally 2D, actually has a depth corresponding the the aperture size and objective used. For fibers with a circular cross section, we have found it most accurate to compare data from individual images. For example, the plane where two layers of fibers connect [Figure 14.9(a)] or the plane going through the middle of the fibers [Figure 14.9(b)] can

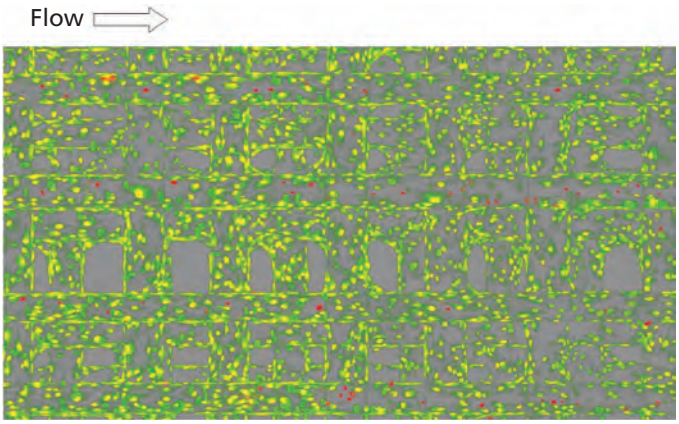

Figure 14.7 Results of confocal imaging. The 3D reconstruction of a confocal microscopy image stack using Zen software. The cells are stained with a modified live/dead assay detailed in Section 14.4.4, in which live cells stain green and dead cells stain red.

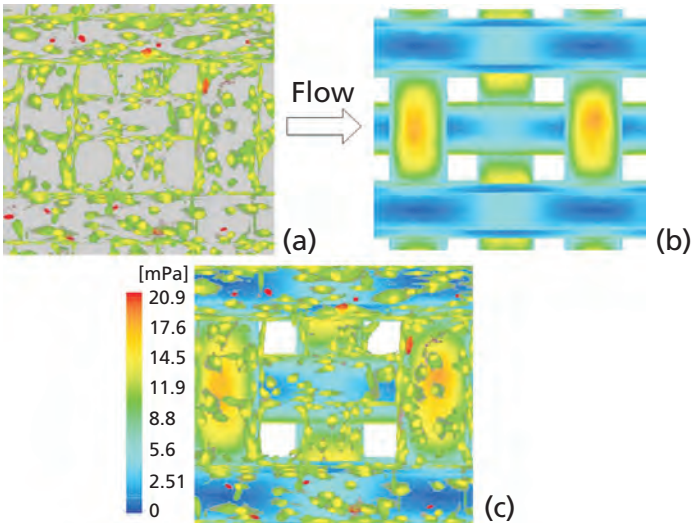

Figure 14.8 Representative output of the method. Focusing on individual pores, (a) the confocal image and (b) the computed shear stress map are overlapped to obtain (c) an image showing the point-by-point correlation between the computational and experimental outputs.

be imaged, and the number of nuclei on fibers running parallel to the flow direction can be compared with fibers running perpendicularly.

Using this microfluidic model, a 3D perfusion environment is obtained that corresponds to an accurately modeled fluid environment within the scaffold pores. By using the described microfluidic chamber, it is possible to actively monitor cell growth and behavior on the scaffold. Varying the fluid flow profile within the 3D environment, qualitative and quantitative changes in cellular activity are monitored, such as changes in cell alignment and protein expression. These changes are seen on the local level and correlated to the local fluid flow environment through the computational model.

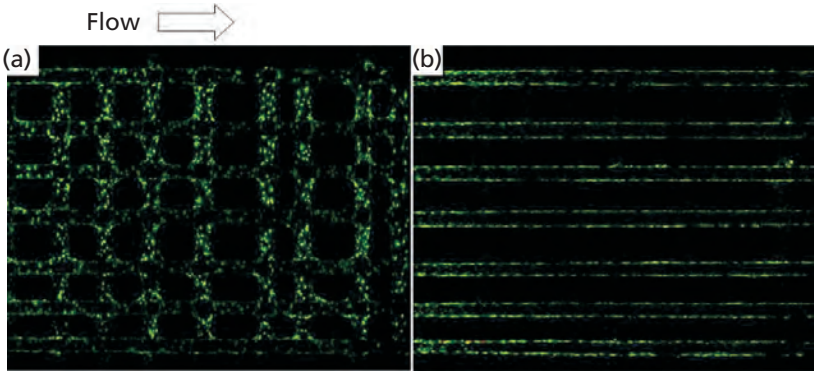

Figure 14.9 Results of confocal imaging. Cross sections, 10 μm thick, of the same scaffold from Figure 14.7. (a) The plane where two levels of fibers meet at 200 μm. (b) The cross section of fibers 250 μm deep.

14.6 Discussion and Commentary

Our target is the development of an integrated experimental/computational microfluidic model for 3D tissue engineering research. Our microfluidic model consists of a microbioreactor in which a thin 3D cellular construct is cultured under interstitial perfusion. The fluidynamics within the scaffold is quantified by a pore-scale CFD simulation, allowing the establishment of correlations between the local field variables calculated for the fluid dynamic field imposed to cells, and the biosynthetic response measured at the cell level during the course of culture.

Pioneering studies by Leclerc et al. [17, 19] established proof of concept for the scalability of the bioreactor approach to microfluidic bioreactors. However, the previous microchanneled chambers used to study the influence of shear stress on cell growth and differentiation simulated a single layer of the channel network and thus were 2D in their logic. The microfluidic model presented here accounts for 3D effects of the actual 3D scaffold structure, which is integrated in the system in several layers. This provides the benefits of controlled microfluidics with more realistic 3D cell culture and computational modeling.

When designing a microfluidic system for your experimental needs, the bioreactor and scaffold used have to be codeveloped in order to ensure accurate operation. Due to experimental constraints, we found it easier to start with design considerations for the scaffold. Fabrication methods, such as spin coating or solvent casting/particulate leaching, provide limited control of the scaffold microstructure. This prevents a realistic prediction of the fluid domain by means of geometrical computational models. The analysis of local field variables of the fluid domain does not allow a point-by-point correlation to what is seen on the actual constructs in this case, instead requiring complex statistical analysis techniques [4, 6, 21]. To ensure a strong correlation with the computational model, it is critical that the scaffold has a tightly controlled geometry. We used polystyrene scaffolds fabricated with a fiber deposition process, which maintains a tightly controlled fiber width as well as accurate fiber placement. While highly accurate and useful for our experiments, this process is limited to fairly basic cross-hatch designs. There are other fabrication methods available to generate more complex controlled microgeometries, such as stereolithography [22, 23].

We chose to use plasma-treated polystyrene as the scaffold material so that the scaffolds were transparent, allowing a greater imaging depth. It is important to be aware of how the microgeometry will affect the imaging quality as well as seeding efficiency and the shear stress profile. The cross-hatch design, with its perpendicular fibers as shown in Figure 14.4, improves seeding efficiency and maximizes the shear stress magnitude extremes. Additionally, this staggered configuration improves imaging, since the microscope does not have to look through a previous fiber layer when looking up to 400 μm in depth. The outer dimensions of the scaffold are dictated by both the microfluidic chamber and microscopy limitations. When using confocal microscopy, the typical imaging depth limit is around 300 μm. Due to the symmetry assumption used in the computational modeling, you need to be able to see at least halfway through the construct. It is for these reasons that we use a scaffold with a 500-μm thickness.

When selecting the flow rates for your bioreactor, you must first determine your upper and lower limits. The upper flow limit is generally given by the rate at which your cells are damaged or washed away. A scaffold with a different surface treatment or microarchitecture could have a higher or lower upper limit. The lower limit for fluid flow is given by a nutrient delivery to the cells and is highly dependent on both the scaffold architecture and the total cell metabolics. Monitoring outlet media with nutrient sensors, such as oxygen, would greatly assist in determining when nutrients become the limiting factor.

The cell-staining protocol is highly dependent on what cellular behavior you are trying to correlate with the fluid environment. You need to balance staining your target with maintaining normal cell behavior. Before any stain is used, you should do an assay to find the optimal exposure level, additionally checking the impact of your scaffold's autofluorescence. For example, we found that we could use DAPI up to a concentration of 10 μg/ml without affecting cell proliferation after 6 days. If you need to refresh your stain during cell culture, you can inject dye into the fluid flow during construct perfusion.

When imaging, there is a balance between image quality and the time required to take the data. We typically use a 10× objective because it has a high enough resolution for our needs and the whole scaffold can be imaged much more quickly when compared to a 20× objective. Two useful features on the LSM 710 system we used were "tile scan" and "auto Z." Tile scan has the microscope acquire a mosaic consisting of partial images, which the software reconstructs to record one complete image of the whole object. Auto Z allows the online modification of acquisition parameters for Z stacks, meaning that the gain increases with an increasing imaging depth, providing images of equal brightness at different depths. Combining z-stacks with tile scan and auto z, you can obtain a high-quality image of the entire scaffold used in the experiment, such as that seen in Figure 14.7.

The computational results determine the scaffold regions characterized by poor or strong fluid-induced mechanical stimulation (i.e., low or high shear stress at the scaffold surfaces). The computed wall shear stresses are an estimate of the shear stresses sensed by cells when adhered at the fiber walls. By using this approach, we assume that the adhered cells have negligible effect on the construct permeability and microgeometry, coherently with other studies [5–8, 24]. This hypothesis is realistic at the initial stage of the culture, from 5 days after seeding up to 2 weeks, depending on the level of cell proliferation and protein synthesis.

In fact, a high cell volume fraction alters the scaffold geometry and affects fluid flow, rendering the computational model inaccurate. Additionally, larger cell clusters with an extracellular matrix will limit the possible imaging depth. Advanced modeling techniques to predict tissue growth in 3D porous scaffolds, accounting for the fluid to structure interaction, have been developed recently [25, 26]. The development of new methods to obtain a more rigorous comparison of experimental measurements with the results obtained from modeling would open new perspectives for the validation of such predictive tools in the field of tissue engineering [27]. Our microfluidic model could potentially be used to monitor volumetric cell growth, allowing for a future dynamic flow analysis that takes into account the changing geometry of the fluid path.

Microfluidic chambers provide a highly controlled platform for acquiring data on cellular behavior under perfusion. Compared to standard culture methods with Petri dishes, microfluidics offer more control, reduced materials, real-time data monitoring, faster cell kinetics, and multiparametric analysis [28]. However, to date, systems generally look at the 2D cell culture with the exception of the 3D cell culture in gels. The methods described here provide the opportunity to combine the benefits of microfluidics with the 3D culture on various cell scaffolds. The computational modeling presented in this chapter allows the user to take full advantage of the fluid control permitted in the bioreactor.

Troubleshooting Table

Problem	Explanation	Potential Solutions
Cells disappear while in the bioreactor.	Cells are dying due to nutrient deficiencies or are being washed away due to high flow rates.	Adjust flow rate.
No fluid flow through a channel.	Misaligned gasket.	Reposition the gasket in relation to the top plate.
Fluid flow between channels.	Fluid pressure is bending the polycarbonate cover on the perfusion chamber.	Add a glass cover slip to the bioreactor between the perfusion chamber and the gasket.
3D image reconstructions look staggered.	The z distance between each image is too great.	The z-distance between images should be less than the image thickness.
Fibers show a polygonal shape after CFD meshing.	Mesh size is too large.	Refine the mesh.
Mesh has distorted elements.	The fluid domain has singularities in correspondence of the upper and lower boundaries.	Eliminate a thin portion of the fluid domain using plane intersections.

14.7 Application Notes

The microbioreactor system outlined in this chapter provides a method for real time, nondestructive data acquisition for cell culture on 3D scaffolds. The system is easily adapted to the equipment present in cell culture labs, with minimal custom components. There exist particularly important examples of applications potentially addressed by the method, in addition to the given example of cell proliferation.

1. The concept of lab-on-a-chip analysis can be applied to 3D tissue enginering with the increased control provided by computational modeling. Arbitrary combinations of environmental factors (e.g., culture media formulation and mechanical stimulation)

can be used to stimulate cells in independent culture chambers to automate analysis of cell response in actual 3D conditions. Examples are the analysis of mesenchymal stem cell (MSC) proliferation, motility, and differentiation in the context of tissue engineering of muskulo-skeletal tissue.

2. Some promising theoretical models of the multiphysic process of tissue growth [25, 26] can be validated by monitoring, in time and space, cell systems cultured in a 3D environment under perfusion.

14.8 Summary Points

1. A microbioreactor system that allows the nondestructive acquisition of data from thin 3D scaffolds with a controlled geometry has been developed. Using appropriate staining protocols, cells on the scaffolds can be monitored in real time.
2. A computational model was developed to quantify the fluidic environment within the scaffold pores. The model boundaries correspond to the environment provided by the microbioreactor system.
3. By combining the computational data with the experimental data, local fluid conditions can be correlated with local cell behavior during the course of culture, in an actual 3D culture environment.

References

[1] Wendt, D., et al, "Uniform Tissues Engineered by Seeding and Culturing Cells in 3D Scaffolds Under Perfusion at Defined Oxygen Tensions," *Biorheology*, Vol. 43, No. 3-4, 2006, pp. 481–488.

[2] Guilak, F., and C. T. Hung, "Physical Regulation of Cartilage Metabolism," in *Basic Orthopaedic Biomechanics and Mechano-Biology*, V. C. Mow and R. Huiskes, (eds.), Philadelphia, PA: Lippincott Williams & Wilkins, 2005, pp. 259–300.

[3] Williams, K. A., S. Saini, and T. M. Wick, "Computational Fluid Dynamics Modeling of Steady-State Momentum and Mass Transport in a Bioreactor for Cartilage Tissue Engineering," *Biotechnology Progress*, Vol. 18, No. 5, 2002, pp. 951–963.

[4] Porter, B., et al., "3D Computational Modeling of Media Flow Through Scaffolds in a Perfusion Bioreactor," *Journal of Biomechanics*, Vol. 38, No. 3, 2005, pp. 543–549.

[5] Singh, H., et al., "Flow Modeling Within a Scaffold Under the Influence of Uni-Axial and Bi-Axial Bioreactor Rotation," *Journal of Biotechnology*, Vol. 119, 2005, pp. 181–219.

[6] Cioffi, M., et al., "Modeling Evaluation of the Fluid-Dynamic Microenvironment in Tissue-Engineered Constructs: A Micro-CT Based Model," *Biotechnology and Bioengineering*, Vol. 93, No. 3, 2006, pp. 500–510.

[7] Boschetti, F., et al., "Prediction of the Micro-Fluid Dynamic Environment Imposed to Three-Dimensional Engineered Cell Systems in Bioreactors," *Journal of Biomechanics*, Vol. 39, No. 3, 2006, pp. 418–425.

[8] Cioffi, M., et al., "Computational Evaluation of Oxygen and Shear Stress Distributions in 3D Perfusion Culture Systems: Macro-Scale and Micro-Structured Models," *Journal of Biomechanics*, Vol. 41, 2008, pp. 2918–2925.

[9] Galbusera, F., et al., "Computational Modeling of Combined Cell Population Dynamics and Oxygen Transport in Engineered Tissue Subject to Interstitial Perfusion," *Computer Methods in Biomechanics and Biomedical Engineering*, Vol. 10, No. 4, 2007, pp. 279–287.

[10] Cartmell, S. H., et al., "Effects of Medium Perfusion Rate on Cell-Seeded Three-Dimensional Bone Constructs In Vitro," *Tissue Eng.*, Vol. 9, 2003, pp. 1197–1203.

[11] Raimondi, M. T., et al., "Mechanobiology of Engineered Cartilage Cultured Under a Quantified Fluid-Dynamic Environment," *Biomechanics and Modelling in Mechanobiology*, Vol. 1, No. 1, 2002, pp. 69–82.

[12] Raimondi, M. T., et al., "The Effect of Media Perfusion on Three-Dimensional Cultures of Human Chondrocytes: Integration of Experimental and Computational Approaches," *Biorheology*, Vol. 41, No. 3-4, 2004, pp. 401–410.

[13] Raimondi, M. T., et al., "The Effect of Hydrodynamic Shear on 3D Engineered Chondrocyte Systems Subject to Direct Perfusion," *Biorheology*, Vol. 43, No. 3-4, 2006, pp. 215–222.

[14] Raimondi, M. T., et al. "Engineered Cartilage Constructs Subject to Very Low Regimens of Interstitial Perfusion," *Biorheology*, Vol. 45, No. 3-4, 2008, pp. 471–478.

[15] Sudo, R., et al., "Transport-Mediated Angiogenesis in 3D Epithelial Coculture," *FASEB Journal*, e-pub 2009.

[16] Sundararaghavan, H. G., et al., "Neurite Growth in 3D Collagen Gels with Gradients of Mechanical Properties," *Biotechnology and Bioengineering*, Vol. 102, No. 2, 2009, pp. 632–643.

[17] Leclerc, E., Y. Sakai, and T. Fujii, "Perfusion Culture of Fetal Human Hepatocytes in Microfluidic Environments," *Biochemical Engineering Journal,* Vol. 20, 2004, pp. 143–148.

[18] Mehta, K., et al., "Quantitative Inference of Cellular Parameters from Microfluidic Cell Culture Systems," *Biotechnology and Bioengineering*, Vol. 103, No. 5, 2009, pp. 966–974.

[19] Leclerc, E., et al., "Study of Osteoblastic Cells in a Microfluidic Environment," *Biomaterials*, Vol. 27, 2006, pp. 586–595.

[20] Wu, H. W., et al., "The Culture and Differentiation of Amniotic Stem Cells Using a Microfluidic System," *Biomedical Microdevices,* e-pub 2009.

[21] Maes, F., et al., "Modeling Fluid Flow Through Irregular Scaffolds for Perfusion Bioreactors," *Biotechnology and Bioengineering*, Vol. 103, No. 3, 2009, pp. 621–630.

[22] Anderson, E. J., and M. L. Knothe Tate, "Design of Tissue Engineering Scaffolds as Delivery Devices for Mechanical and Mechanically Modulated Signals," *Tissue Eng.*, Vol. 13, No. 10, 2007, pp. 2525–2538.

[23] Melchels, F., J. Feijen, and D. Grijpma, "A Poly(D,L-Lactide) Resin for the Preparation of Tissue Engineering Scaffolds by Stereolithography," *Biomaterials*, Vol. 30, 2009, pp. 3801–3809.

[24] Spiteri, C. G., et al., "Substrate Architecture and Fluid-Induced Shear Stress During Chondrocyte Seeding: Role of Alpha5beta1 Integrin," *Biomaterials*, Vol. 29, No. 16, 2008, pp. 2477–2489.

[25] O'Dea, R. D., S. L. Waters, and H. M. Byrne, "A Two-Fluid Model for Tissue Growth Within a Dynamic Flow Environment," *European Journal of Applied Mathematics*, Vol. 19, 2008, pp. 607–634.

[26] Galbusera, F., M. Cioffi, and M. T. Raimondi, "An In Silico Bioreactor for Simulating Laboratory Experiments in Tissue Engineering," *Biomedical Microdevices*, Vol. 10, No. 4, 2008, pp. 547–554.

[27] Hutmacher, D. W., and H. Singh, "Computational Fluid Dynamics for Improved Bioreactor Design and 3D Culture," *Trends in Biotechnology*, Vol. 26, No. 4, 2008, pp. 166–172.

[28] Cimetta, E., et al., "Micro-Bioreactor Arrays for Controlling Cellular Environments: Design Principles for Human Embryonic Stem Cell Applications," *Methods*, Vol. 47, 2009, pp. 81–89.